Indigo carmine removal from aqueous solution using natural biopolymer: fixed-bed column study

Allani C. M. A. Rocha[a], Iara B.Valentim[b], Fabiane C.de Abreu[a,*]

[a] Instituto de Química e Biotecnologia, Universidade Federal de Alagoas (UFAL),
Av. Lourival Melo Mota, s/n, Tabuleiro do Martins, 57072-970, Maceió-AL, Brasil.

[b] Instituto Federal de Educação, Ciência e Tecnologia de Alagoas (IFAL),
Rua Barão de Atalaia, s/n, Poço, 57020-510, Maceió-AL, Brasil.

***Corresponding Authors:**
Fabiane Caxico de Abreu Galdino
E-mail: caxico.fabiane@gmail.com

Abstract

Fixed-bed column studies were conducted, using chitosan and fish scale, to evaluate the removal of Indigo Carmine (IC) from an aqueous solution. The use of scale fish in the adsorption process of IC on scale is reported for the first time and was shown to be influenced by surface treatment. Adsorption of IC on chitosan and fish scale is influenced by initial feed concentration, bed height and flow rate parameters. The adsorption capacities varied from 8 to 13 mg $g^{-1}$for chitosan and from 3 to 14 mg g^{-1} for scale fish. The Adams-Bohart, Thomas, Yan and Yoon-Nelson models were examined in order to predict the breakthrough curves, however none of these models described the experimental data.

Keywords*: adsorption, dye, chitosan, fish scale, fixed-bed column.*

1. Introduction

The discharge of dyes in the environment causes both toxicological and environmental concerns as dyes hamper light penetration, damages the quality of the receiving streams, are toxic to food chain organisms and could be carcinogenic[1,2]. Therefore, the removal of colour from waste effluents is of fundamental importance to the environment [2]. A wide range of methods has been developed for the removal of dyes from wastewaters, such as coagulation, froth flotation, flocculation, adsorption, etc.[3,4]. Amongst these techniques, the adsorption using biosorbents has gained increasing popularity in recent years, as the process produces a high quality treated effluent[5,6].

Among the materials used as biosorbents, chitosan and fish scale has shown to be extremely promising as they are biodegradable, nontoxic biopolymers and residues of the fishing industry [7,8]. Chitosan is produced by deacetylation of chitin, which is found in the skin or shell of anthropods[7]. It is positively charged at pH <6, due to the amino groups dispersed on the protonated structure [9]. Moreover, it is useful as an adsorbent for a large number of pollutants, such as dyes [10,11]and metallic ions [7]. Fish scale is a biocomposite of hydroxyapatite ($Ca_5(PO_4)_3OH$) and highly ordered type I collagen fibrils (main component)[8, 12]. A limited amount of studies have used scales as absorbent, Basu et al. [13,14] and Iqbal et al. [15], investigated the removal of metallic ions using fish scales.

This study investigates the removal of anionic dye (Indigo carmine, IC) from aqueous solution by Chitosan or by fish scale using a fixed bed column. The effect of influent concentration, bed height, and flow rate on the column performance and shape of the breakthrough curves were also evaluated. Kinetic models (Thomas, Adams-Bohart, Yan and Yoon-Nelson) were applied to describe the dynamic performance of the adsorption process.

2. Materials and methods

2.1 Materials and Chemicals

Indigo carmine (IC, Fig. 1) (99 % purity) and glass wool were purchased from Sigma-Aldrich (St. Louis-MO, USA) and used as received. Chitosan (deacetylation degree of 80%) was purchased from TCI-America (Portland, OR, USA). The scales fish (Tambaqui, Colossoma macropomum) were collected at the municipal market of Maceió, Alagoas. A glass mini-column with 0.6 cm internal diameter and length of 9 cm was employed.

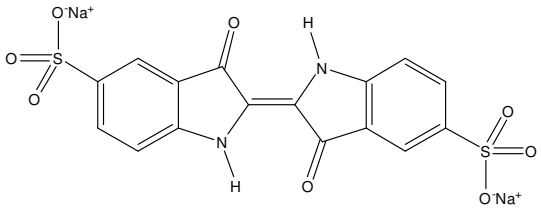

Fig. 1. Chemical structure of IC.

2.2 Processing of the biosorbents

Chitosan was used as received. The fish scales were washed numerous times with distilled water and left in contact with a sodium hydroxide solution at pH 9.0 for 4h. Subsequently, this medium was immersed in an ultrasonic bath for 1h, the scales were separated and washed with distilled water numerous times and left to dry at 60 °C in an oven for 6 h. Soon after, they were ground into the processor and separated on 18 mesh sieve obtaining a dry powder. This powder (without treatment) was inserted in the column and used as a biosorbent in the sorption experiments. Other columns were prepared to evaluate the efficiency of this

biosorbent after washing it first with acid solution (HCl) at pH 1.5 for 20 min, then acid solution (HCl) at pH 4.5 for 20 min and acidifying the dye solution with HCl until reaching a pH of 3.0.

2.3Characterization of biosorbents

Textural characterization (BET surface area, pore volume and pore size) of the Chitosan and the fish scale were measured by a surface area and porosity analyzer (Autosob I,Quantachrome Corporation, USA) using N_2 adsorption at 77K. In addition, the surface functional groups of the chitosan and the fish scale (before and after adsorption of IC) were detected by Fourier Transform Infrared (FTIR) spectrophotometer(FTIR-2000, Perkin Elmer). Before each analysis, the samples were dried at 60 °C for 72 h. The spectra were recorded from 4000 to 400cm^{-1}.The surface area characterization of chitosan, and fish scales are shown in **Table 1**.

Table 1

Typical physical properties of Chitosan and fish scales adsorbents.

	Chitosan	Fish Scales
BET surface area (m^2g^{-1})	0.97	3.65
Langmuir surface area (m^2g^{-1})	1.47	5.33
Average pore diameter (Å)	84.24	113.12
Total pore volume (cm^3g^{-1})	0.0026	0.0117

2.4 Fixed bed adsorption studies

Continuous flow adsorption studies were conducted in a glass column. A glass wool plug was used at the bottom to support the adsorbent bed as well as to prevent leakage of adsorbent. Another glass wool plug was used on top of the bed to prevent overflow of the adsorbent, as showed in the Fig. 2. The adsorbent bed heights used were1, 3 and 6 cm, in a column with a 0.6 cm internal diameter. Dye solution of known concentrations (10, 15 and 20 mg L^{-1}) was pumped through the column at a desired flow rate (4 and 8 mL min^{-1}) controlled by a peristaltic pump (model BP 200). Effluent concentrations of IC were monitored by measuring their absorbance at 609 nm, using the same spectrophotometer. Samples were collected periodically until maximum color dye intensity was reached ($C/C_0 \geq 0.9$). Breakthrough curves were constructed as C/C_0vs. time. All the experiments were carried out at room temperature (298 ± 1 K).

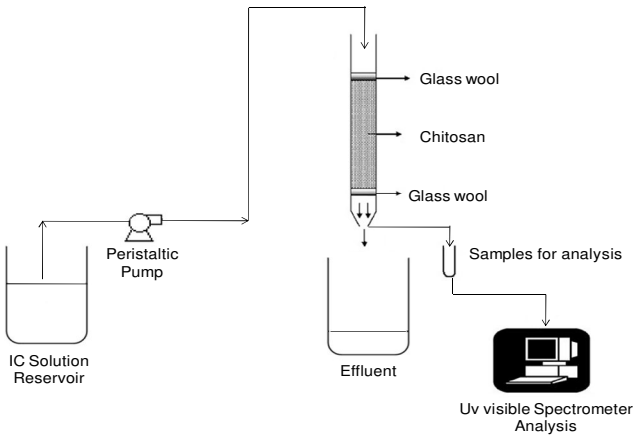

Fig. 2. Schematic disposition of the experimental set up for fixed bed studies.

2.5 Evaluation of data

The column flow data was evaluated using various models of non-linear regression analysis using the software package STATISTICA 7 for Windows. The following mathematical models were used: Thomas [16], Adams-Bohart [17], Yan [18] and Yoon-Nelson [19] models.

Thomas model

The Thomas model obeys Langmuir kinetics of sorption-desorption with no axial dispersion, and it assumes that the rate driving force obeys second-order reversible reaction kinetics[20, 21, 22]. The model has the following equation:

$$\frac{C}{C_O} = \frac{1}{1+\exp\left(\frac{k_{TH}\cdot q_T \cdot m}{Q} - \frac{k_{TH}\cdot C_O}{Q}\cdot V\right)} \quad (1)$$

where, C is effluent concentration (mg L^{-1}) at time t, C_O is initial concentration (mg L^{-1}), k_{TH} is Thomas rate constant, (L min^{-1} mg^{-1}), q_T is maximum adsorption capacity (mg g^{-1}), m is mass of the adsorbent (g), V is effluent volume (mL) and Q is flow rate (mL min^{-1}). The value of time, $t=V/Q$. The constants k_{TH} and q_T are determined from a plot of C/C_O against t for a given set of conditions using non-linear regression analysis.

Adams-Bohart model

The model assumes that equilibrium is not instantaneous, and the adsorption rate is proportional to residual capacity of the sorbent and the concentration of the sorbing species. This model is used for the description of the initial part of the breakthrough curve [23, 24, 25, 26, 27]. The fundamental equation that describes the relationship between C/C_O and t in a flowing system is given by:

$$\frac{C}{C_O} = \frac{1}{1+\exp\left(\frac{N_O\cdot k_{AB}\cdot Z}{v} - k_{AB}\cdot C_O \cdot t\right)} \quad (2)$$

where, N_0 is the adsorption capacity of the bed (mg L^{-1}), k_{AB} is Adams-Bohart rate constant (L min^{-1} mg^{-1}), Z is the bed height (cm), ν is the linear flow rate (cm min^{-1}) and t is the time (min).

Yan model

Yan et al. [18] developed a new model for heavy metal removal in a biosorption column. This new model could overcome the drawback in the Thomas Model, in particular its lack in predicting the effluent concentration at time zero. The fundamental equation for this model is expressed in the following form:

$$\frac{C}{C_O} = 1 - \frac{1}{1+\left(\frac{Q^2\cdot t}{K_Y\cdot q_Y\cdot m}\right)^{\left(\frac{K_Y\cdot C_O}{Q}\right)}} \quad (3)$$

Where, k_y is the kinetic rate constant for Yan Model (L min^{-1} mg^{-1})and q_y is the maximum adsorption capacity (mg g^{-1}) of adsorbent estimated by Yan Model.

Yoon-Nelson model

Yoon and Nelson [19] developed a relatively simple model. This model does not require detailed data regarding the characteristics of adsorbate, the type of adsorbent, and the physical properties of adsorption bed. The rate of decrease in the probability of adsorption for each adsorbate molecule is proportional to the probability of adsorbate adsorption and to the probability of adsorbate breakthrough on the adsorbent. The fundamental equation for this model is expressed in the following form:

$$\frac{C}{C_O} = \frac{\exp\left(K_{YN} \cdot t - \tau \cdot K_{YN}\right)}{1 + \exp\left(K_{YN} \cdot t - \tau \cdot K_{YN}\right)} \quad (4)$$

where, k_{YN} is Yoon-Nelson rate constant (min^{-1}) and τ is the time required for 50% of adsorbate breakthrough (min).

The results of IC adsorption on the chitosan or fish scale using a continuous system were presented in the form of breakthrough curves which showed the ratio of the outlet IC concentration (C) to the inlet IC concentration (C_0) as a function of time (C/C_ovs. t). Equilibrium dye uptake in the column or maximum capacity [28, 1, 24] of the column (q_{eq}, mg g^{-1}) was calculated using Eq. (1):

$$q_{eq} = \frac{Q}{1000 \times X} \int_{t=0}^{t=t_{total}} C_{ad}\, dt \quad (1)$$

Where X is the mass of adsorbent in g, C_{ad} (mg L^{-1}) is the adsorbed IC concentration ($C_{ad} = C_o - C$), Q is the volumetric flow rate (L min^{-1}) and t_{total} is the total flow time (min^{-1}).

3. Results and discussion

3.1 Treatment of fish scales

The adsorption of IC on fish scales was analyzed using fixed bed column, obtained C/C_0 as a function of time to evaluate the efficiency of this biosorbent, under three distinguishing conditions: (a) untreated fish scales, (b)after acid-treated packing column (pH 1.5 and 4.5), and(c) by acidification of the dye solution (pH 3.0) before passing through the column. Figure 3 shows breakthrough curves for IC adsorption on fish scale under these conditions. Under conditions (a) and (b), the fish scale bed was exhausted in the shortest time (< 60 min) leading to the earliest breakthrough. Under condition (c), an extended breakthrough curve was obtained indicating that a higher volume of the solution could be treated at a saturation time of 200 min. This condition was chosen for all experiments.

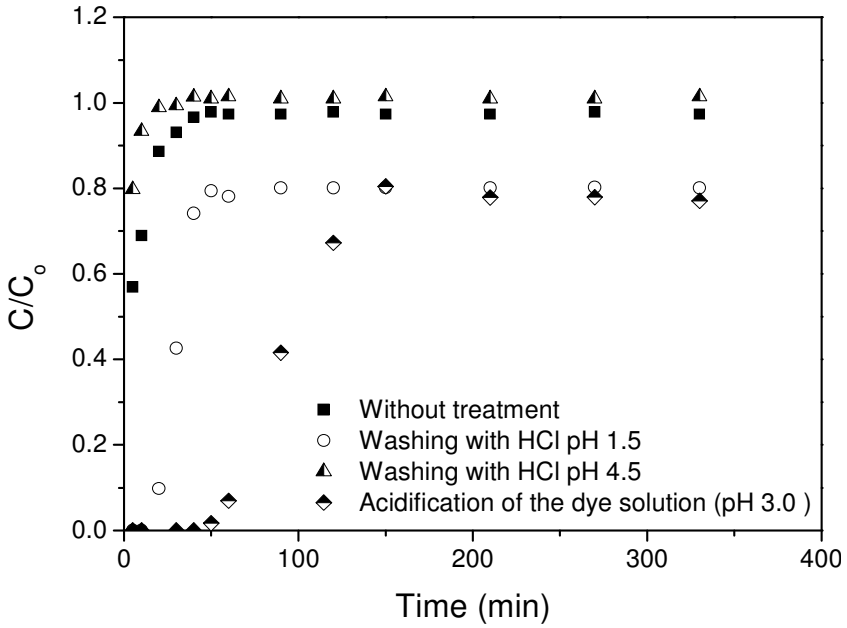

Fig. 3. Breakthrough curves (C/C_0 vs. time) for IC adsorption on fish scale at three distincting conditions: fish scale untreated, fish scale treated with an acid solution (pH 1.5 and 4.0), and the acidification of the dye solution (pH 3.0). C_0 = 15 mg L^{-1}, bed height of 3 cm, flow rate=4 mL min^{-1} and T =298 ±1K)

The FTIR spectra of fish scale with and without previous contact with an acid solution, in the range of 4000-400 $cm^{-1}$are shown in Fig. 4. The characteristic absorption bands of fish scale are: 3500 cm^{-1} corresponding to hydroxyl groups, three bands at 1653, 1567 e 1242 cm^{-1}attributed to amides I, II and III of type I collagen, respectively, and absorption bands at 1000 and 600 cm^{-1}corresponding to phosphate groups in the apatite lattice [8]. Similar results were described by Ikoma et al. [8] where it was concluded that fish scale is a nanocomposite consisting of type I collagen and calcium-deficient apatite containing carbonate ions. After careful drying, the IR spectrum of the acidified fish scale was similar to the fish scale IR spectrum before contact with the acid solution. However, an increase in the intensity of the absorption bands, especially those corresponding to hydroxyl groups, along with a change in the pattern of bands between 1700 – 1200 cm^{-1} were observed, suggesting that a modification took place on the scale surface. Experiments were then conducted with acidified dye solutions (pH 3.0), which has proven to be very effective in the adsorption process.

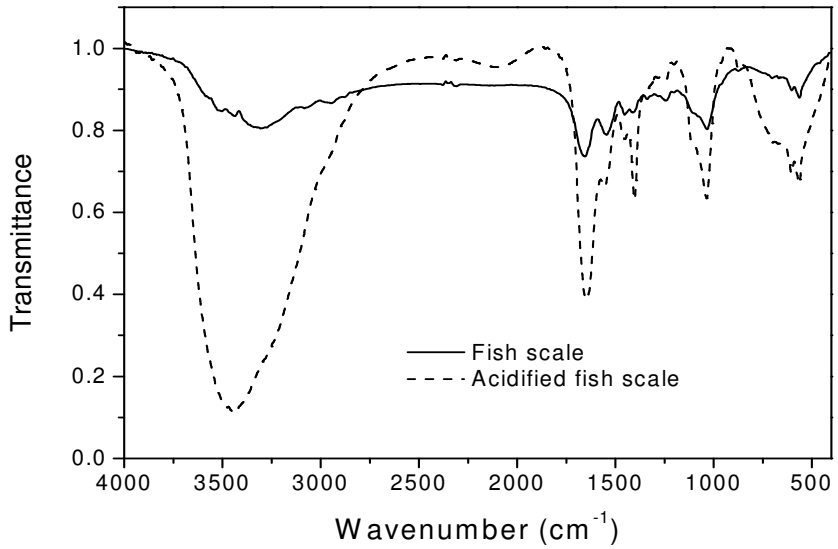

Fig. 4. FTIR spectra of fish scales with and without previous contact with an acid solution (pH 3.0).

The intensity increase of the broad band corresponding to hydroxyl groups is explained by Zanaboni et al. [29]. In an acid medium, the type I collagen fibrils are not formed because the interactions of the triple helices are disrupted. Thus, there is structural exposure and, consequently, the aminoacids are more prone to undergo chemical reactions. The fish scale became positively charged and the amount of hydroxyl groups increased, according to the following reaction:

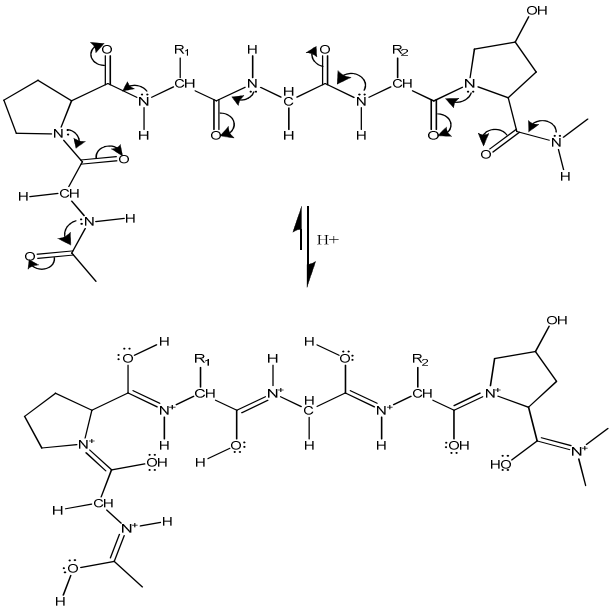

Fig. 5. Scheme representing the effect of the addition of acid on the chemical structure of fish scale.

3.2Influence of operating conditions on fixed bed adsorption of IC

Operational parameters such as initial feed concentration, bed height and flow rate are important for column design. The effects of these parameters on the adsorption of the IC ontochitosan and ontofish scales were studied and illustrated in Fig. 6. Figures 6a and 6d show that the change in the IC's initial concentration has a significant effect on the breakthrough curve. These results demonstrate that an increase in concentration causes an expected decrease in the saturation time, i.e., the binding sites are more rapidly

saturated in the column [25]. For the lowest concentration, an extended breakthrough curve is obtained, therefore, a higher volume of the solution is treated. Similar trends were obtained for adsorption of basic dye using activated carbon prepared from oil palm shell [1], removal of As (III) ions from aqueous solution [26] and removal of lead (II) by adsorption using treated granular activated carbon [25].

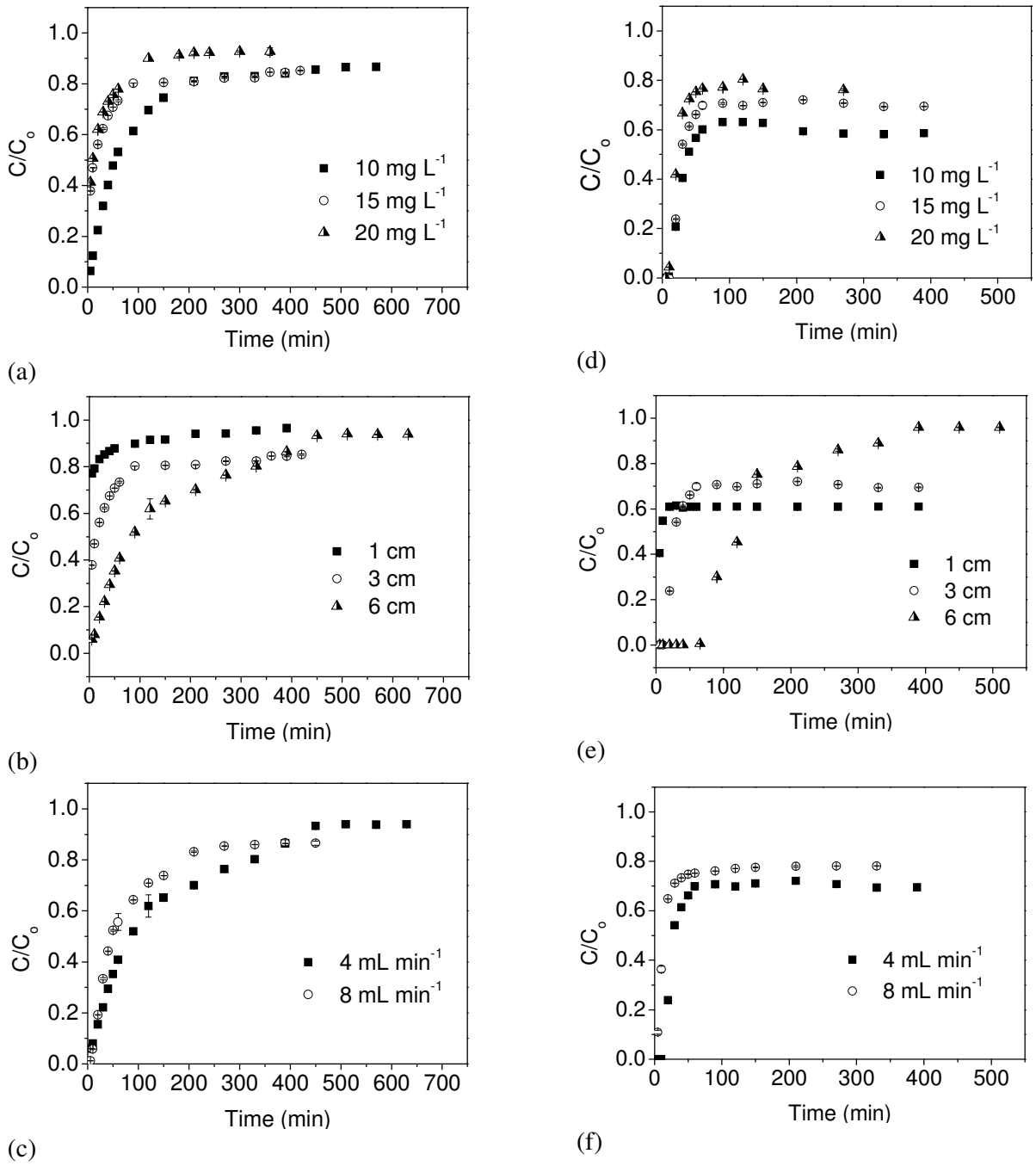

Fig. 6. Breakthrough curves (C/C_0 vs. time) for IC adsorption on chitosan (a-c) and fish scale (d-f): (a) and (d) different initial dye concentrations (bed height 3 cm, flow rate = 4 mL min^{-1}, temperature 298±1 K); (b) and (e) different bed heights (initial dye concentration = 15 mg L^{-1}, flow rate = 4 mL min^{-1}, temperature = 298±1 K); (c) and (f) different flow rates (initial dye concentration = 15 mg L^{-1}, bed height 6 cm for chitosan and 3 cm for scale, temperature 298±1 K).

Figures 6b and 6e present the breakthrough curve obtained for IC adsorption on the chitosan and fish scale, respectively, for different bed heights of 1, 3 and 6 cm at a constant flow rate of 4 mL min^{-1} and an IC initial concentration of 15 mg L^{-1}. The results show that the saturation time increases as bed height increases, therefore a greater volume is treated. The effect of the flow rate (4 and 8 mL min^{-1}) was investigated using a constant adsorbent bed height of 6 cm to chitosan and 3cm to fish scale and the initial dye concentration of 15 mg L^{-1}, as shown by the breakthrough curve in Figs. 6c and 6f. As expected, an increase in flow rate produces a diminution in saturation time, consequently, the curves become steeper with a shorter mass transfer zone.

Table 2 shows the column parameters obtained for IC adsorption on chitosan and fish scale in different IC initial concentrations, bed heights and flow rates at 298 K.

According to Muhamad et al. [20], the adsorption capacity decreases with increase of the initial concentration due to the exhaustion of the sorption sites available on solid. Our results are consistent with the literature, except for fish scale in the concentration of 15 mg L^{-1} which provided an adsorption capacity about 14 mg g^{-1}. To evaluate the parameters bed height and flow rate, an initial concentration at 15 mg L^{-1} was fixed (Table 2). It was observed that the adsorption capacity for both biosorbents decreased with the decrease in bed height. Futalan et al. [30] affirm that when the bed height is reduced the solute does not have enough time to diffuse into the whole of the adsorbent mass, because the mechanism that governs the mass transfer is the axial dispersion. At higher flow rate, the contact time between the adsorbate and adsorbent is minimized, leading to lower adsorption capacity, as shown in Table 2.

Table 2

Column parameters of the IC adsorption on chitosan and on fish scale at different IC initial concentrations, bed heights and flow rates.

Chitosan				
Initial IC concentration (mg L^{-1})	Bed height (cm)	Flow rate (mL min^{-1})	Saturation time (min)	Adsorption capacity q_e (mg g^{-1})
10	3	4	570	13
15	3	4	420	12
20	3	4	360	10
15	1	4	120	8
15	6	4	630	13
15	6	8	330	11
Fish Scale				
Initial IC concentration (mg L^{-1})	Bed height (cm)	Flow rate (mL min^{-1})	Saturation time (min)	Adsorption capacity q_e (mg g^{-1})
10	3	4	330	12
15	3	4	270	14
20	3	4	150	10
15	1	4	60	9
15	6	4	510	15
15	3	8	210	3

Adsorption capacities of both solids are similar (Table 2), although the fish scales have a surface area and a pore volume larger than that of chitosan (Table 1). This suggests that fish scale showed a performance as good as chitosan. Infrared analyses were performed before and after the adsorption of IC on adsorbents (Figure 7). It is noted that the intensities of the absorption bands of the solids decreases after adsorption of the dye especially those corresponding to hydroxyl groups, suggesting that the dye is present on the surface of the solids. There is also a large contribution of these groups in the adsorption process which are more accentuated for fish scale. Figure 8 shows various possibilities for interaction between IC and adsorbent (chitosan (a) [31] and fish scale (b)).

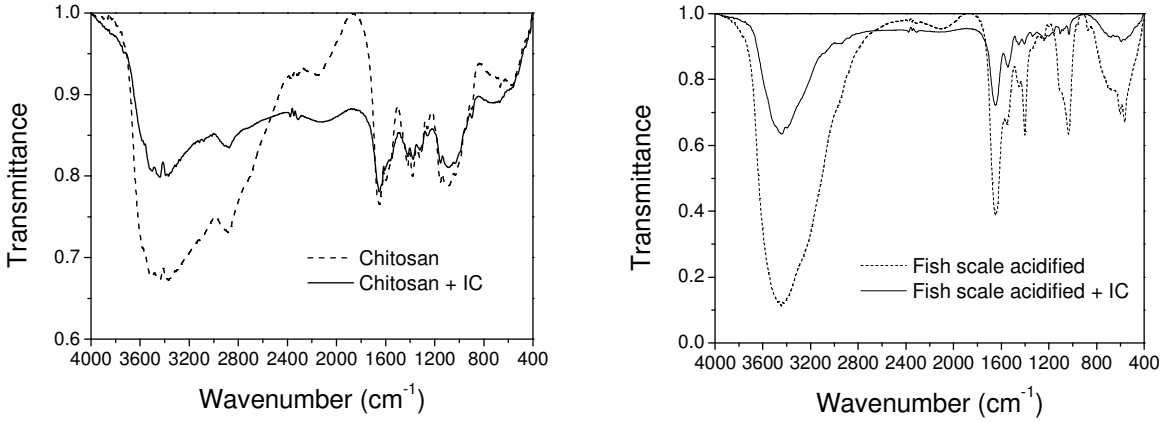

(a) (b)

Fig. 7. Infrared spectra of the (a) chitosan and chitosan-IC; (b) fish scale acidified and fish scale acidified-IC

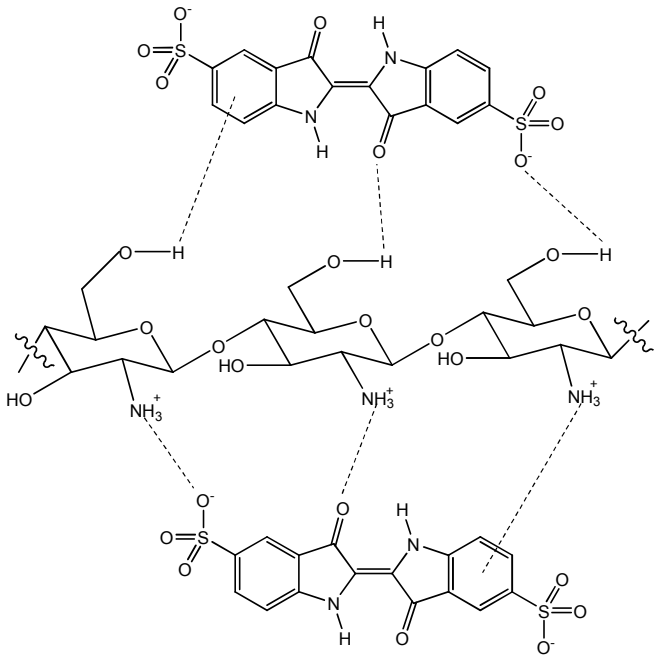

(a)

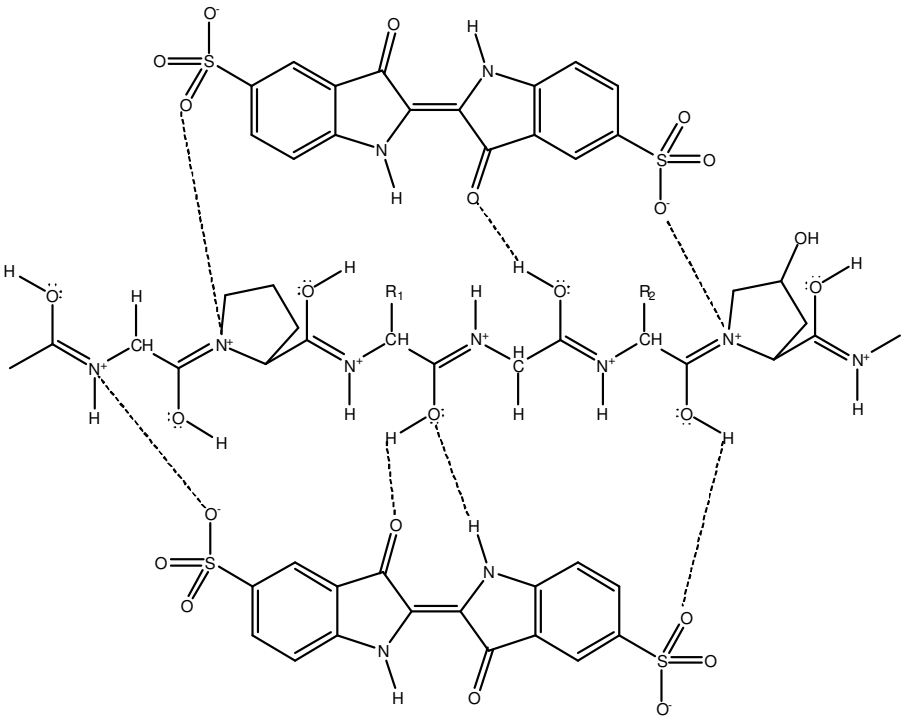

(b)

Fig. 8. Some possible interactions between (a) IC and chitosan; (b)IC and fish scale.

3.3 Model of column data

To predict the breakthrough curves, four models were used: Adams-Bohart, Thomas, Yan and Yoon-Nelson. The data fit by these models were examined using the correlation coefficients (R^2) and comparing the q values (Tables 2, 3 and 4).

Tables 3 and 4 show the adsorption capacity of chitosan and fish scale for IC, respectively, as well as model constants estimated by the Adams-Bohart, Thomas, Yan and Yoon-Nelson models. Comparing the correlation coefficients (R^2) obtained from the models for chitosan and fish scales (Tables 3 and 4), it is possible to observe that the best model to represent the data of adsorption of IC on chitosan was Yan, however, none of the models was suitable to represent the adsorption of IC on fish scale. Comparing the values of q (calculated in Table 1 and experimental in Table 2 and 3), it is clear that none of the models could adequately describe the adsorption of IC on both solids.

Table 3

Parameters obtained from the non-linear fit breakthrough data for IC adsorption on chitosan at different initial IC concentrations, bed heights and flow rates (298±1 K).

Thomas Model					
Initial IC concentration (mg L^{-1})	Bed height (cm)	Flow rate (mL min^{-1})	q_T (mg g^{-1})	k_{TH} (L mg^{-1} min^{-1})	R^2
10	3	4	9.4	1.6	0.914
15	3	4	10.1	0.3	0.815
20	3	4	1.6	1.3	0.940
15	1	4	112.4	0.4	0.942
15	6	4	10.0	0.7	0.961
15	3	8	5.8	1.3685	0.937
Adams-Bohart Model					
Initial IC concentration (mg L^{-1})	Bed height (cm)	Flow rate (mL min^{-1})	N_o (mg/L)	k_{AB} (L mg^{-1} min^{-1})	R^2
10	3	4	3677	1.6×10^{-3}	0.914
15	3	4	3977	0.4×10^{-3}	0.815
20	3	4	629	1.4×10^{-3}	0.940
15	1	4	45008	0.05×10^{-3}	0.942
15	6	4	4299	0.8×10^{-3}	0.961
15	3	8	250	13.8×10^{-3}	0.937
Yan Model					
Initial IC concentration (mg L^{-1})	Bed height (cm)	Flow rate (mL min^{-1})	q_Y (mg g^{-1})	k_Y (L mg^{-1} min^{-1})	R^2
10	3	4	0.1	4×10^{-4}	0.996
15	3	4	0.3	1×10^{-4}	0.988
20	3	4	0.3	1×10^{-4}	0.995
15	1	4	2.5	1×10^{-4}	0.984
15	6	4	0.2	3×10^{-4}	0.996
15	3	8	0.1	6×10^{-4}	0.994
Yoon-Nelson Model					
Initial IC concentration (mg L^{-1})	Bed height (cm)	Flow rate (mL min^{-1})	τ (min)	k_{YN} (min^{-1})	R^2
10	3	4	78.3	1.62×10^{-2}	0.914
15	3	4	56.4	0.50×10^{-2}	0.815
20	3	4	6.7	2.51×10^{-2}	0.940
15	1	4	213.0	0.67×10^{-2}	0.942
15	6	4	122.1	1.12×10^{-2}	0.961
15	3	8	71.1	2.05×10^{-2}	0.937

Table 4

Parameters obtained from the non-linear fit breakthrough data for IC adsorption on fish scales at different initial IC concentrations, bed heights and flow rates (298±1 K).

Thomas Model					
Initial IC concentration (mg L^{-1})	Bed height (cm)	Flow rate (mL min^{-1})	q_T (mg g^{-1})	k_{TH} (L mg^{-1} min^{-1})	R^2
10	3	4	5.9	0.8	0.553
15	3	4	8.8	0.5	0.599
20	3	4	4.5	3.8	0.819
15	1	4	12.0	0.3	0.513
15	6	4	7.7	2.0	0.987
15	3	8	1.2	0.5	0.571
Adams-Bohart Model					
Initial IC concentration (mg L^{-1})	Bed height (cm)	Flow rate (mL min^{-1})	N_o (mg/L)	k_{AB} (L mg^{-1} min^{-1})	R^2
10	3	4	7140	0.4×10^{-5}	0.553
15	3	4	5383	0.5×10^{-5}	0.599
20	3	4	2741	3.8×10^{-5}	0.819
15	1	4	7349	0.3×10^{-5}	0.513
15	6	4	4903	2.0×10^{-5}	0.987
15	3	8	716	0.5×10^{-5}	0.571
Yan Model					
Initial IC concentration (mg L^{-1})	Bed height (cm)	Flow rate (mL min^{-1})	q_Y (mg g^{-1})	k_Y (L mg^{-1} min^{-1})	R^2
10	3	4	0.1	2×10^{-4}	0.845
15	3	4	0.2	2×10^{-4}	0.874
20	3	4	0.3	3×10^{-4}	0.923
15	1	4	0.1	1×10^{-4}	0.795
15	6	4	0.4	8×10^{-4}	0.996
15	3	8	0.2	4×10^{-4}	0.885
Yoon-Nelson Model					
Initial IC concentration (mg L^{-1})	Bed height (cm)	Flow rate (mL min^{-1})	τ (min)	k_{YN} (min^{-1})	R^2
10	3	4	152.0	0.0042	0.5535
15	3	4	76.5	0.0068	0.5986
20	3	4	29.2	0.0760	0.8188
15	1	4	34.8	0.0039	0.5130
15	6	4	139.2	0.0293	0.9870
15	3	8	10.2	0.0076	0.5712

Dos Anjos et al [10] investigated the interaction of IC with chitosan using a bath procedure and concluded that both Langmuir and Freundlich adsorption models were suitable to explain experimental data. The Langmuir model alone is not able to describe the interaction of IC with chitosan, due to its complexity. None of the models used in this study were adequate to describe the experimental data obtained in the fixed bed column, possibly because most models are based on the Langmuir model. It is known that the surface of chitosan has adsorption sites energetically different similar to ammonium, acetyl, and hydroxyl groups. Similar to chitosan, the experimental data of IC onfish scales was not able to be described by any of the used models, suggesting that the creation of a novel model would be more adequate when analysing kinetic columnx for IC removal.

4. Conclusions

The removal of IC in a fixed-bed column system using chitosan and fish scale as an adsorbent is an effective and feasible method. In an acid medium, the intensities of the absorption bands of fish scale corresponding to hydroxyl groups increased. After the adsorption process, the absorption bands of both solids decrease especially those corresponding to hydroxyl groups, suggesting that these groups contribute to the adsorption process. Adsorption of IC on chitosan and fish scales depends on initial feed concentration, bed height and flow rate. An increase in initial concentration and flow rate causes a decrease on saturation time and an increase in bed height increases saturation time. Adsorption capacities of both solids are similar, although the fish scales have a surface area and a pore volume larger than that of chitosan. None of the models used were adequate to describe the experimental data obtained for both solids in fixed bed column, suggesting that column kinetics for IC removal could be described more adequately by a new model to be studied.

Acknowledgements

The financial support by the Brazilian agencies CNPq, CAPES/PNPD, PADCT/CNPq, FAPEAL, CNPq/PNPD (process 559277/2008-3) and RENORBIO is greatly acknowledged.

References

[1] Tan IAW, Ahmad A L, Hameed BH. Desalination 2008; 225; 13-28.

[2] Elemen S, Kumbasar EPA, Yapar S. Dyes and Pigments 2012; 95; 102-111.

[3] Elemen E, Cserháti T, Oros G. Environment International 2004; 30; 953-971.

[4] Mezohegyi G, Zee FPVD, Font J, Fortuny A, Fabregat A. Journal of Environmental Management 2012; 102; 148-164.

[5] Sze MFF, Lee VKC, McKay G. Desalination 2008; 218; 323-333.

[6] Asgher M. Water Air Soil Pollut 2012; 223; 2417–2435.

[7] Ngah WSW, Teong LC, Hanafiah MAKM. Carbohydrate Polymers 2011; 83; 1446–1456.

[8] Ikoma T, Kobayashi H, Tanaka J, Walsh D, Mann S. International Journal of Biological Macromolecules 2003; 32; 199–204.

[9] Prado AGS, Torres JD, Faria EA, Dias SCL. Journal of Colloid and Interface Science 2004; 277; 43–47.

[10] Anjos FSC, Vieira EFS, Cestari AR. Journal of Colloid and Interface Science 2002; 253; 243–246.

[11] Fan L, Li M, Lv Z, Sun M, Luo C, Lu F, Qiu H. Colloids and Surfaces B: Biointerfaces 2012; 95; 42 - 49.

[12] Chen S, Ikoma T, Ogawa N, Migita S, Kobayashi H, Hanagata, N. Science and Technology of Advanced Materials 2010; 11; 1-4.

[13] Basu, A, Rahaman MS, Islam MR. Canadian Journal of Chemical Engineering 2011; 89; 499-507.

[14] Basu, A, Rahaman, MS, Mustafiz S, Islam MR. Journal of Environmental Engineering And Science 2007; 6; 455-462.

[15] Iqbal, J, Tirmizi AS, Mirza ML, Iqbal J. Journal Of The Chemical Society Of Pakistan 2005; 27; 77-81.

[16] Thomas HC. Contributtion from the Department of Chemistry of Vale University 1944; 66; 1664-1666.

[17] Bohart, GS, Adams EQ. Behavior of Charcoal Toward Chlorine 1920; 523-544.

[18] Yan G, Viraraghavan T, Chen M. Adsorption Science & Technology 2001; 19; 25-43.

[19] Yoon YH, Nelson JH. Am IndHygAssoc J 1984; 45; 509-16.

[20] Muhamad H, Doan H, Lohi A. Chemical Engineering Journal 2010; 158; 369-377.

[21] Sivakumar P, Palanisamy PN. Indian Journal of Chemical Technology 2009; 16; 301-307.

[22] Vijayaraghavan K, Prabu D. Journal of Hazardous Materials 2006; B137; 558–564.

[23] lkoc E,Nuhoglu Y, Dundar M.Adsorption of chromium (VI) on pomace—an olive oil industry waste: batch and column studies.Journal of Hazardous Materials 2006; B138; 142-151.

[24] Wang X, Kim JH, Min BG. Fibers and Polymers 2008; 9; 263-266.

[25] Goel, J, Kadirvelu K, Rajagopal C, Garg VK. J Hazard Mater 2005; B125; 211-20.

[26] Singh TS, Pant KK. Separation and Purification Technology 2006; 48; 288–296.

[27] Quintelas C, Silva B, Figueiredo H, Tavares T. Biodegradation 2010; 21; 379-392.

[28] Lodeiro P, Herrero R, Vicente MES. Journal of Hazardous Materials 2006; B137; 244-253.

[29] Zanaboni G,Rossi A,Onana AMT,Tenni R. Matrix Biology2000; 19; 511-520.

[30] Futalan CM, Kan C, Dalida ML, Pascua C, Wan M. Carbohydrate Polymers2011; 83; 697–704.

[31] Chatterjee S, Chatterjee S, Chatterjee BP, Guha AK. Colloids and Surfaces A: Physicochem. Eng. Aspects, 2007; 299; 146–152.